ChemPubSoc Europe

DOI: 10.1002/syst.201900038

CHEMSYSTEMSCHEM Articles

VIP *Very Important Paper*

Special Collection

Chemically Fuelled Self-Regulating Gel-to-Gel Transition

Santanu Panja, Bart Dietrich, and Dave J. Adams*[a]

Artificial self-regulating materials can be prepared by exploiting fuel-driven pathways. Dynamic covalent bonds are formed and broken reversibly under mild reaction conditions. Herein, we utilise this concept to programme a system that can undergo a fuel-driven self-regulated gel-to-gel transition. The reaction between the gelator and the fuel resulted in a change in chemical structure of the gelator that initially causes a transition from a solution to gel state by co-assembly. With time, the intermediate complex collapses, re-forming the gelator structure. However, the gel does not collapse. This method allows us to prepare gels with improved mechanical strength. Unlike conventional gel-to-gel transitions, exploitation of dynamic covalent chemistry provides an opportunity to access materials that cannot be prepared directly under similar final conditions.

1. Introduction

Fuel-driven pathways as a means of bond formation and rupturing has emerged as an extremely powerful strategy for bio-mimicry as well as for the synthesis of functional materials.[1] Amongst functional materials, supramolecular hydrogels are important soft materials with many multifunctional applications.[2] Supramolecular gels are formed by the self-assembly of small monomeric building blocks into long fibrous structures by non-covalent interactions, followed by trapping of the solvent by the networks. In spite of the presence of a large volume of liquid, these materials behave as viscoelastic solids. As the non-covalent interactions prevailing in gel architectures are individually weak and reversible, it is possible to perturb the intermolecular associations to adapt gel properties.[3] In a related fashion, fuel-driven pathways can also be used to form and break covalent bonds reversibly under mild reaction conditions[1a] and therefore can be used to prepare gels with a high degree of control over the final gel properties during a sol-to-gel transition.[1d,i,4]

In general, gels are prepared first as a static system and then explored for various target specific applications. In this context, post-assembly modification of the gel networks can be used to prepare new functional materials. Gel-to-gel transformations can be used to modify gel properties, and are usually accomplished by manipulating a pre-gel network by using stimuli like pH, ions or irradiation.[3b,c,f,5] Dynamic covalent bond formation can also be used to induce post-assembly modifications in a gel-to-gel fashion.[6] However, post-assembly fabrication usually relies on external input or specific input from the user, often alters the final conditions, and imposes chemical changes on the gelator structure.[3b,c,f,5–6]

One potential way to counter these issues is to devise a method where modification of the gelator molecules is carried out at the beginning of gelation in such a way that the modified molecules have a pronounced effect on the aggregation. Hence, in the early stages, the gel state incorporates the modified molecules. With time, the modified molecules revert to the original precursor keeping the assembled structure intact. This would be an interesting strategy to compare gel properties under similar final conditions. To achieve this aim, here we describe a chemically fuelled self-regulating dynamic system that undergoes a pre-programmed gel-to-gel transition through successive covalent bond formation and rupture (Figure 1). Reaction between the gelator and the fuel resulted in a change in chemical structure of the gelator that initially causes a transition from a solution to a gel state by co-assembly. With time, the intermediate complex begins to collapse, re-forming the precursor. The complete cycle resulted in an autonomous gel-to-gel transformation with the actual gelator structure at the end. We show that the final properties of the gel differ significantly from those of the gel obtained directly from the gelator in absence of the fuel. Exploitation of this fuel-driven pathway results in formation of a different type of gel network at the end with improved mechanical properties of the gels.

2. Results and Discussion

Amphiphile **1** undergoes self-aggregation in DMSO-H_2O (20/80, v/v) and forms a self-supporting gel at a concentration of 4 mg/mL (minimum gelation concentration, mgc) or above (Figure S10). The pH of the gel was measured to be pH 4.5. Confocal microscopy imaging shows the existence of densely packed needle-like fibres in the gel state (Figure 2a). Note that drying artefacts are common in these self-assembled gel systems[7] and so we avoid using techniques such as TEM where drying is required. The mechanical properties of the gel were

[a] *Dr. S. Panja, Dr. B. Dietrich, Prof. D. J. Adams*
School of Chemistry
University of Glasgow
Glasgow, G12 8QQ (UK)
E-mail: dave.adams@glasgow.ac.uk

Supporting information for this article is available on the WWW under https://doi.org/10.1002/syst.201900038

An invited contribution to a Special Collection on Systems Chemistry Applied to Materials Science

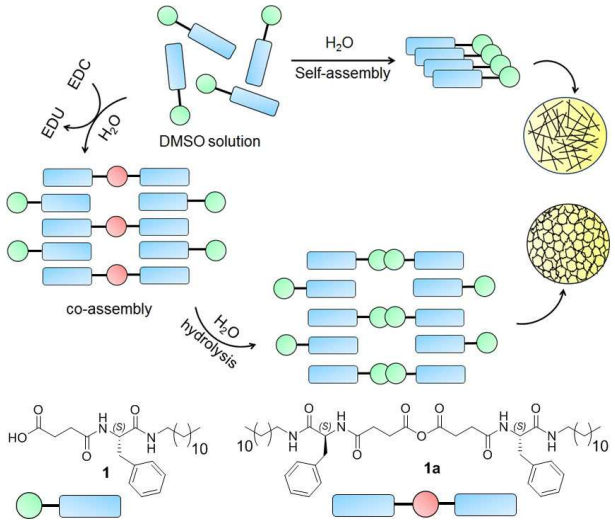

Figure 1. Cartoon representing gel-to-gel transition with autonomous regulation. The gelator used here (**1**) can form a self-supporting gel. On treatment with EDC, **1** is converted to its anhydride (**1 a**) which is also capable of forming a gel by co-assembly with **1**. With time, hydrolysis of **1 a** results in regeneration of **1** resulting in a gel-to-gel transformation with a different final fibre network.

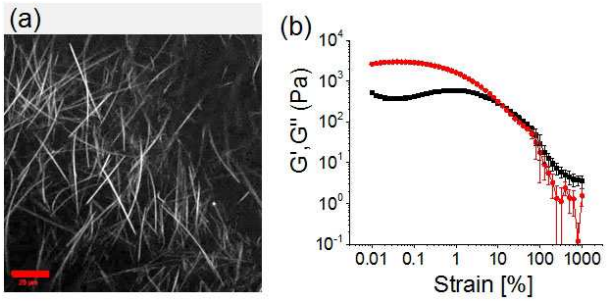

Figure 2. (a) Confocal fluorescence microscopy image (the scale bar represents 20 μm) and (b) strain sweep experiment of the hydrogel of **1** (the red data represents G′ and the black data G″). In both cases, the concentration of **1** is 4 mg/mL and solvent is 20/80 DMSO/water (v/v).

examined by rheology. The materials were found to have considerably higher values of the storage modulus (G′) as compared to the corresponding loss modulus (G″) (Figure 2b, S11). The gel starts to break at a low strain of ~0.5% (the critical strain) after which it completely converted to a sol after ~12% strain (the yield point). The rheological moduli (G′ and G″) are independent of frequency. At a concentration of **1** below the mgc, precipitation occurred instead, but aggregated structures could be imaged by confocal microscopy (Figure S12).

To construct a self-regulating gel-to-gel transition involving **1**, we utilized the carbodiimide-induced acid-anhydride reversible conversion as the key chemical reaction (Figure 1). We used 1-ethyl-3-(3-dimethylaminopropyl)carbodiimide (EDC) as the chemical fuel to convert **1** into its anhydride **1 a**. We preferred to use EDC over DCC (N,N′-dicyclohexylcarbodiimide) because of its high solubility in water as well as the urea obtained as by-product after the reaction is also water soluble. EDC has been extensively used as fuel reaction for constructing transient hydrogel systems.[8] However, in most of the cases, either a labile alcohol was added to form the metastable ester[8e] or a dicarboxylate was converted into cyclic anhydride.[8b,d] Important work in this area has been carried out by the groups of Boekhoven, Hartley and Das amongst others.[8–9]

As a first step to realize the EDC-induced chemical changes of **1**, we added 0.5 molar equivalents of an aqueous solution of EDC to a DMSO solution of **1** at a concentration of 1 mg/mL such that the final ratio of DMSO/water was 20/80. Interestingly, instead of the precipitation which occurs for **1** alone at this concentration (Figure S10), initially we obtained a translucent gel (Figure 3a). After 15 minutes, the gel showed a transition to a highly viscous solution. Over longer times, precipitation occurred. These visual observations suggest the formation of a transient hydrogel. By varying the concentration of EDC, we can easily control the lifetime of the transient gel (Figure 3a). In all cases, HRMS spectra recorded after freeze-drying the gel states confirm the existence of both the anhydride (**1 a**) and the acid (**1**), and hence endorse the co-assembly induced gelation (Figure S13). Alongside this, HRMS spectra of the solution states demonstrate complete hydrolysis of **1 a** to the acid (**1**). The anhydride **1 a** is more hydrophobic than **1**, and hence the formation of **1 a** leads to changes in aggregation by co-assembly with **1**. After this, slow hydrolysis of **1 a** to **1** leads to the destruction of the co-assembled structures and results in conversion to a sol.

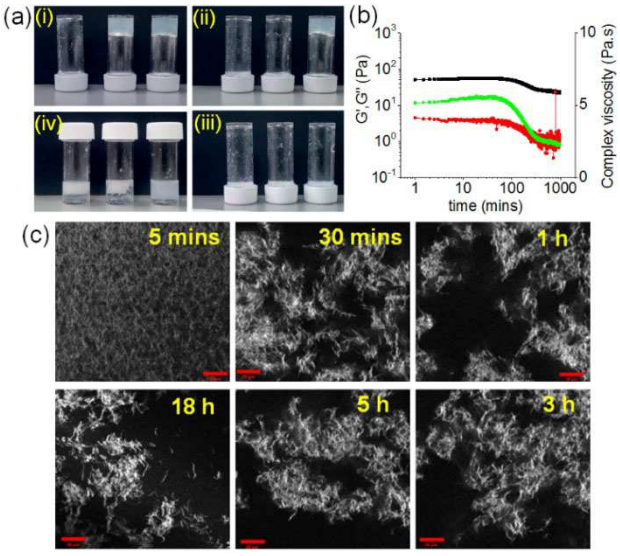

Figure 3. (a) Photographs showing the phase change of **1** with time when an aqueous solution of EDC was added to the mixture of **1** in DMSO. Photographs taken after (i) 5 mins, (ii) 15 mins, (iii) 1 h, (iv) 18 h. In each photograph, from left to right, the initial concentration of EDC is 0, 0.5, and 1.0 molar equivalents with respect to **1**. (b) Variation of G′ (black), G″ (red) and complex viscosity (green) with time for **1** in the presence EDC-fuelled reaction. (c) Time-dependent confocal microscopy images of **1** in the presence of EDC-fuelled reaction (scale bars represent 20 μm). For (a)–(c), the initial concentration of **1** is 1 mg/mL and solvent is 20/80 DMSO/water (v/v). For (b) and (c), the initial concentration of EDC is 0.5 molar equivalent with respect to **1**.

We followed this process using rheology. Initially, the storage modulus (G′) was considerably higher than the loss modulus (G″), indicating that a gel was formed rapidly in the presence of EDC (Figure 3b). With time, the hydrolysis of anhydride becomes predominant and the gel started to collapse resulting in a decrease in the rheological moduli. Importantly, an increase in EDC concentration resulted in a considerable delay in the decrease of both G′ and G″ (Figure S14), agreeing with the observed physical behaviour (Figure 3a). Viscosity data recorded with time are also consistent with rheological changes demonstrating gradual transformation of highly viscous materials to the considerably less viscous solutions (Figure 3b and S14). Note that, during the gel-to-sol transitions, there were no crossover between G′ and G″ in both cases because of the formation of a colloidal suspension. Frequency sweep experiments of the solutions obtained after ~18 hours of the addition of EDC show that these are structured liquids (Figure S15). Interestingly, when we performed the same reaction using DCC (N,N′-dicyclohexylcarbodiimide) instead of EDC, no transient hydrogel formation occurred. This is presumably due to poor solubility of DCC in the prescribed medium (Figure S16, S17) that did not allow formation of sufficient anhydride required for gelation.

The resulting gel-to-sol transitions were further examined by confocal studies (Figure 3c, S18). Time dependent confocal microscopy imaging reveals formation of densely packed fibres in the early stages. These fibres are engaged to form a net type network. With time, the density of the net-like structures decreases, and spherulitic aggregates were formed. Higher stability for the interlinked net-type fibres was observed at high EDC concentration. We note that there was a significant difference in the microstructure of the solution directly obtained from **1** in the absence of EDC (Figure 3c, S12, S18). There was also slight decrease in the viscosity of the solution (Figure S19).

To trigger an autonomous gel-to-gel transition, we performed the same reactions at a higher gelator concentration (4 mg/mL). As expected, a stable gel was formed quickly when a solution of EDC (0.5 or 1 equimolar) was added to the DMSO solution of **1** (Figure 4a). Time sweep rheology shows the formation of gels at early stages that evolve with time (Figure 4b and Figure S18). A similar trend in the variation of G′ and viscosity was found in presence of 0.5 equimolar of EDC, as observed at lower gelator concentrations (see above). However, a significant difference in gelation kinetics was observed at higher EDC concentration, where a slow decrease in rheological moduli as well as viscosity was monitored over time (Figure S20). Frequency sweep data shows that gels are formed at the end (Figure S21) unlike the liquids formed at lower concentration.

Time dependent confocal microscopy imaging showed the formation of fibres and a high density of net-type microstructures throughout the whole process in both cases (Figure 4c and Figure S22). HRMS spectra collected on freeze-dried samples at different times again confirm the formation of anhydride and regeneration of the acid (Figure S23). Interestingly, under both conditions, the gel structures persist at the

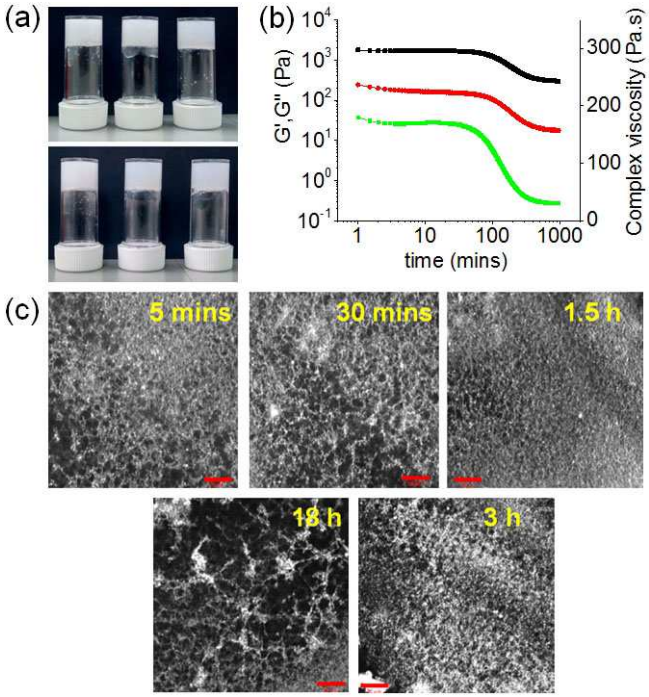

Figure 4. (a) Photographs showing the hydrogels of **1** prepared in DMSO-water either in the absence or presence of EDC; (top) after 5 mins and (bottom) after 18 h. In each photograph, from left to right, the initial concentration of EDC is 0, 0.5, and 1.0 molar equivalent with respect to **1**. (b) Variation of G′ (black), G″ (red) and complex viscosity (green) with time for **1** in the presence EDC fuelled reaction. (c) Time-dependent confocal microscopy images of **1** in the presence of EDC fuelled reaction (scale bars represent 20 μm). For (a)–(c), the initial concentration of **1** is 4 mg/mL and solvent is 20/80 DMSO/water (v/v). For (b) and (c), the initial concentration of EDC is 0.5 molar equivalents with respect to **1**.

end (Figure 4a). No significant change in the visual appearance of the final gels was found in comparison to the gel directly obtained from DMSO-H_2O without using EDC (Figure 4a). However, a significant difference in microstructure of the final gels was observed (Figure 2a, 4c, S22). Instead of the formation of needle structures as in the absence of EDC, here we obtained gels that exhibited net-like fibre arrangements in both cases. Although slight variation in the pH change of the medium was noticed during the EDC-fuelled reactions, no significant difference in the pH of the final gels was observed (pH 4.3–4.4) (Figure S24). Throughout the process, no visual sol formation occurred. Hence, the chemically fuelled dynamic self-assembly here leads to an unusual self-directed gel-to-gel transition.

To monitor the evolution of the gels further, emission spectra were recorded. For the experiments, we incorporate 20 μL of 0.005 M pyrene solution into the DMSO solution of **1** prior to the addition of EDC (0.5 or 1 equimolar) and recorded the change in emission intensity of pyrene with time. In both cases, as soon as EDC solutions were added, a strong emission at 390 nm appeared along with a weak shoulder at 473 nm (Figure S25). The emission at 390 nm and 473 nm correspond to the monomer and excimer emission of pyrene respectively.[10] The variation of intensity of the peaks with time depends upon the initial concentration of EDC. The increased emission at

390 nm can be ascribed to a more hydrophobic environment being formed, which changes as the reaction proceeds. The structures formed must be responsible for the underlying network since in the case of 0.5 equimolar of EDC, the plot of intensity at 390 nm against time showed a similar trend as that of the rheology and viscosity (Figure 5a). On the other hand, in presence of 1 equimolar of EDC, the intensity at 390 nm increases slowly at the early stages and became almost constant after 1.5 h (Figure S26). This difference compared to the 0.5 equivalents of EDC suggests that the underlying structures depend on the amount of EDC used.

Comparison of emission of pyrene recorded in absence and presence of **1** reveals that irrespective of initial EDC concentration, the emission of pyrene was quenched significantly in the gel states (in presence of **1**) compared to in the solution state (in absence of **1**) (Figure S27). Moreover, a gradual increase in initial EDC concentration resulted in gels where the monomer emission of pyrene progressively increases. In this context, UV-vis spectra of the final gels further correlate different molecular packing in the aggregated states (Figure 5b, S28). In UV-vis, the absorption signatures of pyrene at 320 nm and 338 nm were suppressed in the gel obtained without using EDC. In comparison, both the EDC fuelled gels showed shoulders at 320 nm and 338 nm. Interestingly, both the peaks become more prominent for the gel obtained from higher EDC concentration. These data suggest a difference in underlying molecular packing in structures underlying the gels formed without EDC and those formed in the presence of EDC. However, an exact determination of the packing is highly challenging. For example, FTIR spectra of different gels were recorded after freeze-drying to determine the molecular packing, but no significant change in the stretching frequency of the acid carbonyl group was observed (Figure S29). This implies that the changes may be subtle, or that drying has resulted in the same new structure being formed in each case.

The final mechanical properties of the gels depend upon the initial reaction conditions (Figure 5c, S21, Table S1). An increase in EDC concentration from 0.5 equivalents to 1 equivalent resulted in ~3-fold increase in stiffness (G′) of the gel. It also causes a substantial increase in gel strength (~5 times). We suggest that as different concentrations of EDC are added, the co-assemblies formed by the anhydride are kinetically trapped, which would agree with differences in the pyrene fluorescence data (above). Energy dissipation from these kinetically-trapped states through hydrolysis governs the final properties of the gels.[9b] In comparison to the gel directly obtained from DMSO-water, the self-regulated gels exhibited a lower gel stiffness (Table S1), but, irrespective of initial EDC concentrations, the self-regulated gels could withstand considerably higher strains (4–20 times increase in gel strength) as well as high crossover points (yield points are >100% strain where G″>G′). We suggest that highly interlinked net-type fibres can withstand a higher stress compared to the unbranched needle-type fibres. Our self-triggered gel-to-gel approach therefore leads to the formation of gels with improved mechanical strength as compared to the original material. It also provides opportunity to access materials that cannot be prepared directly under similar final conditions.

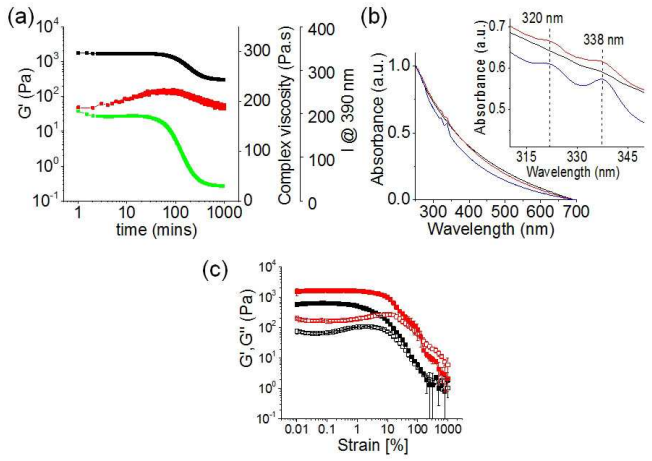

Figure 5. (a) Variation of G′ (black), complex viscosity (green) and emission intensity (red) with time for **1** from the EDC fuelled reaction involving initial conditions: [**1**] = 4 mg/mL, [EDC] = 1.0 equiv. The emission intensity of pyrene ($c = 4.95 \times 10^{-5}$ M) was measured with time in the presence of **1**. (b) Normalized absorption spectra of the hydrogels of **1** (after ~18 h) prepared under different conditions. Initial conditions: [**1**] = 4 mg/mL, [pyrene] = 4.95×10^{-5} M, [EDC] = 0 equiv. (black), 0.5 equiv. (red) and 1.0 equiv (blue). Inset represents the expanded section of (b). (c) Strain sweep experiments of the hydrogels of **1** obtained from EDC fuelled reactions involving initial conditions: [**1**] = 4 mg/mL, [EDC] = 0.5 equiv (black data) and 1.0 equiv (red data). The closed symbols represent G′, the open symbols G″. For (a)–(c), the solvent is 20/80 DMSO/water (v/v).

3. Conclusions

In conclusion, we have successfully designed a fuel-driven dynamic system that undergoes an unusual gel-to-gel transition with autonomous regulation. To construct the dynamic system, we utilized the carbodiimide-induced acid-anhydride reversible reaction as a key step. Unlike conventional gel-to-gel transitions, exploitation of fuel-driven pathways leads to an automated gel-to-gel system at similar final conditions, whilst the final properties of the gels can be controlled by simply varying the fuel concentration. Our method allows us to prepare gels with improved mechanical strength as compared to the initially formed materials. We envisage that this approach will open up new opportunities to synthesize self-programmed tunable materials.

Acknowledgements

SP thanks the Royal Society and SERB of India for a Newton International Fellowship. DA thanks the EPSRC for a Fellowship (EP/L021978/1), which also funded BD.

Conflict of Interest

The authors declare no conflict of interest.

Keywords: chemical fuels · fuel-driven pathway · gel-to-gel transition · hydrogels · self-regulation

[1] a) S. J. Rowan, S. J. Cantrill, G. R. L. Cousins, J. K. M. Sanders, J. F. Stoddart, *Angew. Chem. Int. Ed.* **2002**, *41*, 898–952; *Angew. Chem.* **2002**, *114*, 938–993; b) J. Jiang, Y. Zhao, O. M. Yaghi, *J. Am. Chem. Soc.* **2016**, *138*, 3255–3265; c) C. S. Hartley, J. S. Moore, *JACS* **2007**, *129*, 11682–11683; d) C.-W. Chu, L. Stricker, T. M. Kirse, M. Hayduk, B. J. Ravoo, *Chem. Eur. J.* **2019**, *25*, 6131–6140; e) Y. Zhang, M. Barboiu, *Chem. Rev.* **2016**, *116*, 809–834; f) P. Dydio, P.-A. R. Breuil, J. N. H. Reek, *Isr. J. Chem.* **2013**, *53*, 61–74; g) M. Matache, E. Bogdan, N. D. Hădade, *Chem. Eur. J.* **2014**, *20*, 2106–2131; h) H. Wang, Z. Zeng, P. Xu, L. Li, G. Zeng, R. Xiao, Z. Tang, D. Huang, L. Tang, C. Lai, D. Jiang, Y. Liu, H. Yi, L. Qin, S. Ye, X. Ren, W. Tang, *Chem. Soc. Rev.* **2019**, *48*, 488–516; i) J.-Y. Zhang, L.-H. Zeng, J. Feng, *Chin. Chem. Lett.* **2017**, *28*, 168–183.

[2] a) J. Mayr, C. Saldías, D. Díaz Díaz, *Chem. Soc. Rev.* **2018**, *47*, 1484–1515; b) P. Dastidar, *Gels* **2019**, *5*, 15; c) N. Mehwish, X. Dou, Y. Zhao, C.-L. Feng, *Mater. Horiz.* **2019**, *6*, 14–44; d) T. Christoff-Tempesta, A. J. Lew, J. H. Ortony, *Gels* **2018**, *4*, 40; e) J. Li, L. Geng, G. Wang, H. Chu, H. Wei, *Chem. Mater.* **2017**, *29*, 8932–8952; f) A. Panja, K. Ghosh, *New J. Chem.* **2019**, *43*, 934–945.

[3] a) S. Panja, D. J. Adams, *Chem. Commun.* **2019**, *55*, 10154–10157; b) W. Zhang, C. Gao, *J. Mater. Chem. A* **2017**, *5*, 16059–16104; c) A. Panja, K. Ghosh, *Mater. Chem. Front.* **2018**, *2*, 1866–1875; d) C. Echeverria, S. N. Fernandes, M. H. Godinho, J. P. Borges, P. I. P. Soares, *Gels* **2018**, *4*, 54; e) M. D. Segarra-Maset, V. J. Nebot, J. F. Miravet, B. Escuder, *Chem. Soc. Rev.* **2013**, *42*, 7086–7098; f) W. Tanaka, H. Shigemitsu, T. Fujisaku, R. Kubota, S. Minami, K. Urayama, I. Hamachi, *J. Am. Chem. Soc.* **2019**, *141*, 4997–5004.

[4] a) Q. An, I. D. Wessely, Y. Matt, Z. Hassan, S. Bräse, M. Tsotsalas, *Polym. Chem.* **2019**, *10*, 672–678; b) D. A. Fulton, *Supramolecular Amphiphiles* **2017**, 150–168; c) J. Boekhoven, J. M. Poolman, C. Maity, F. Li, L. van der Mee, C. B. Minkenberg, E. Mendes, J. H. van Esch, R. Eelkema, *Nat. Chem.* **2013**, *5*, 433; d) F. Picchioni, H. Muljana, *Gels* **2018**, *4*, 21; e) P. Sun, S. Ren, A. Wu, N. Sun, L. Shi, L. Zheng, *Chem. Commun.* **2019**, *55*, 9861–9864.

[5] a) E. R. Draper, T. O. McDonald, D. J. Adams, *Chem. Commun.* **2015**, *51*, 12827–12830; b) H. Frisch, P. Besenius, *Macromol. Rapid Commun.* **2015**, *36*, 346–363; c) S. Khan, S. Sur, P. Y. W. Dankers, R. M. P. da Silva, J. Boekhoven, T. A. Poor, S. I. Stupp, *Bioconjugate Chem.* **2014**, *25*, 707–717.

[6] a) S. J. Beckers, S. Parkinson, E. Wheeldon, D. K. Smith, *Chem. Commun.* **2019**, *55*, 1947–1950; b) Y. Ge, H. Gong, J. Shang, L. Jin, T. Pan, Q. Zhang, S. Dong, Y. Wang, Z. Qi, *Macromol. Rapid Commun.* **2019**, 1800731; c) C. Liang, S. Kulchat, S. Jiang, J.-M. Lehn, *Chem. Sci.* **2017**, *8*, 6822–6828; d) K. Imato, T. Ohishi, M. Nishihara, A. Takahara, H. Otsuka, *J. Am. Chem. Soc.* **2014**, *136*, 11839–11845.

[7] L. L. E. Mears, E. R. Draper, A. M. Castilla, H. Su, Zhuola, B. Dietrich, M. C. Nolan, G. N. Smith, J. Doutch, S. Rogers, R. Akhtar, H. Cui, D. J. Adams, *Biomacromolecules* **2017**, *18*, 3531–3540.

[8] a) M. Tena-Solsona, C. Wanzke, B. Riess, A. R. Bausch, J. Boekhoven, *Nat. Commun.* **2018**, *9*, 2044; b) M. Tena-Solsona, B. Rieß, R. K. Grötsch, F. C. Löhrer, C. Wanzke, B. Käsdorf, A. R. Bausch, P. Müller-Buschbaum, O. Lieleg, J. Boekhoven, *Nat. Commun.* **2017**, *8*, 15895; c) B. Zhang, I. M. Jayalath, J. Ke, J. L. Sparks, C. S. Hartley, D. Konkolewicz, *Chem. Commun.* **2019**, *55*, 2086–2089; d) B. Rieß, C. Wanzke, M. Tena-Solsona, R. K. Grötsch, C. Maity, J. Boekhoven, *Soft Matter* **2018**, *14*, 4852–4859; e) S. Bal, K. Das, S. Ahmed, D. Das, *Angew. Chem. Int. Ed.* **2019**, *58*, 244–247.

[9] a) L. S. Kariyawasam, C. S. Hartley, *J. Am. Chem. Soc.* **2017**, *139*, 11949–11955; b) R. K. Grötsch, C. Wanzke, M. Speckbacher, A. Angı, B. Rieger, J. Boekhoven, *J. Am. Chem. Soc.* **2019**, *141*, 9872–9878.

[10] N. M. Cox, L. P. Harding, J. E. Jones, S. J. A. Pope, C. R. Rice, H. Adams, *Dalton Trans.* **2012**, *41*, 1568–1573.

Manuscript received: August 26, 2019
Version of record online: November 4, 2019

